Taylor & Francis
Taylor & Francis Group

A subspace trust-region method for seismic migration inversion

Zhenhua Li[a,b] and Yanfei Wang[a]*

[a]Key Laboratory of Petroleum Resources Research, Institute of Geology and Geophysics, Chinese Academy of Sciences, Beijing 100029, People's Republic of China; [b]Graduate University, Chinese Academy of Sciences, Beijing 100049, People's Republic of China

In seismic exploration, regularized migration inversion of seismic data usually requires solving a weighted least-squares problem with constrains. It is well known that directly solving this problem using some decomposition techniques is very time-consuming, which makes it less possible for practical use. For iterative methods, previous research is mainly on solving the inverse model in a full space. In this paper, a robust subspace method is applied to seismic migration inversion with Gaussian beam representations of Green's function. The problem is first formulated by incorporating regularizing constraints, and then, it is changed from full space to subspace and solved by a trust-region method. To test the potential of the application of the developed method, synthetic data simulations are performed. The results show that this method is very promising for ill-posed seismic migration inversion problems.

Keywords: subspace method; seismic inversion; migration; trust-region method; Gaussian beam

AMS Subject Classifications: 86-08; 65J15; 65N21; 90C30

1. Introduction

Seismic migration is the core of reflection seismology. How to solve ill-posed inverse problems is one of the key problems in it. At present, seismic migration usually only yields an image of the positions of geological structures, and it has invalid information for subsequent lithology analysis and attributes extraction. To get an image with true amplitude, we suggest that seismic inversion should be performed. In seismic migration, the reflectors are imaged, in the sense that its position and shape are more correctly represented, but there is no attempt to recover information about the material parameters of the subsurface. This difference represents the major distinction between 'migration' and 'inversion' [2]. However, this distinction has blurred in recent years as the more modern methods to migration do attempt to address the amplitude issue. Some migration algorithms could handle relative amplitudes correctly in an inversion sense. We call those, which use inversion techniques in migration to achieve true amplitude and high resolution, seismic migration inversion.

---

*Corresponding author. Email: yfwang@mail.iggcas.ac.cn

Seismic migration inversion is usually described by the following equation [2]:

$$d(\mathbf{x}_g, \mathbf{x}_s, \omega) = \omega^2 \int_{\mathbf{\Omega}} \frac{R(\mathbf{x})}{v^2(\mathbf{x})} [G(\mathbf{x}, \mathbf{x}_s, \omega) + d(\mathbf{x}, \mathbf{x}_s, \omega)] G(\mathbf{x}, \mathbf{x}_g, \omega) \, d\mathbf{x}, \tag{1}$$

where $d(\mathbf{x}, \mathbf{x}_s, \omega)$ is the scattered field, $R(\mathbf{x})$ is the reflectivity model and $G(\mathbf{x}, \mathbf{x}_g, \omega)$ is called Green's function. It is nonlinear because it has a term that contains the product of the unknown reflectivity model $R(\mathbf{x})$ and the unknown field $d(\mathbf{x}, \mathbf{x}_s, \omega)$. However, in geophysical sense, it is reasonable to assume that the scattered field $d(\mathbf{x}, \mathbf{x}_s, \omega)$ is significantly smaller than the incident field $G(\mathbf{x}, \mathbf{x}_s, \omega)$. Therefore, the linearized version of Equation (1) can be written as the following equation:

$$d(\mathbf{x}_g, \mathbf{x}_s, \omega) = \omega^2 \int_{\mathbf{\Omega}} \frac{R(\mathbf{x})}{v^2(\mathbf{x})} G(\mathbf{x}, \mathbf{x}_s, \omega) G(\mathbf{x}, \mathbf{x}_g, \omega) \, d\mathbf{x}. \tag{2}$$

According to Equation (2), we can form the following operator equation by combining all the observation data over every pair $(\mathbf{x}_g, \mathbf{x}_s)$:

$$\mathbf{d} = \mathcal{L}(R(\mathbf{x})). \tag{3}$$

If an harmonic solution of Green's function is adopted, the seismic migration inversion can be efficiently performed by FFT (Fast Fourier Transform) or GRT (Generalized Randon Transform). However, using this kind of method will generate great error when an inaccurate velocity model is used or the depth is large. It would sound very good if we can find an exact inverse operator for $\mathcal{L}$ at a low cost. However, in geophysics, this is a typical ill-posed problem and the discrete matrix of $\mathcal{L}$ is singular; therefore, the inverse can hardly be determined. Alternatively, assuming L is the discrete matrix of $\mathcal{L}$, there are several solutions in practice:

(1) Conjugate approximation:

$$F = L^{\mathrm{T}}.$$

Note that conjugate approximation is the simplest form to approximate the inverse. However, inversion according to it does not take into account the influence of coherent noise and neglects amplitude errors due to losses and truncation. In some cases, the inverse can be very different from the transpose, which will result in bad imaging quality. This method is almost always used in practical situations because of its simplicity and efficiency.

(2) The inversion of the significant values in the eigen-value spectrum of a forward modelling matrix:

$$F = Y D_c^{-1} X^{\mathrm{T}},$$

where $L = XDY^{\mathrm{T}}$. This is called the singular value decomposition of L [6]. Matrix D is a diagonal matrix containing the eigen-values of D and matrix D_c^{-1} contains the inverted eigen-values of which exceed a pre-specified threshold: all eigen-values smaller than this threshold are set to zero. Hence, in F, the very small eigen-values are not inverted but set to zero. The efficiency and accuracy would be the two main tricky problems when this method is applied to very large-scale seismic data.

(3) Least-squares inversion [7]:

$$F = [L^{\mathrm{T}}L]^{-1}L^{\mathrm{T}}.$$

We must declare the drawbacks of this operation [14]: (1) $[L^{\mathrm{T}}L]^{-1}$ is much more ill-posed than L, thus $[L^{\mathrm{T}}L]^{-1}$ is highly sensitive to the perturbations in data; (2) huge computational cost.

(4) Tikhonov regularization migration:

$$F = [L^{\mathrm{T}}L + \alpha\Omega]^{-1}L^{\mathrm{T}},$$

where Ω represents the normalized spatial autocorrelation matrix of the noise and α equals the signal-to-noise ratio for one temporal frequency component [15]. For white noise, $\Omega = I$. It may also turn to be very time-consuming when the scale of the problem becomes large.

As analysed above, all the present seismic migration inversion schemes have their own drawbacks. In this paper, we firstly build up a new model for migration inversion to get better imaging result. In this forward model, we do not use harmonic solution, but represent Green's function by a summation of Gaussian beams which can tackle with multiple arrivals and eliminate caustic problem. Then, we accelerate the inversion using a subspace trust-region method. The subspace method originated from optimization theory and is implanted into seismic migration inversion for the first time. In Section 4, numerical examples are presented and followed by some discussion.

2. Seismic migration inversion

We cannot expect to solve the linear system (3) by algebraic strategy easily, because the discrete matrix of $\mathcal{L}$ is usually badly conditioned. In addition, the noise and the band-limited effect cannot be ignored when the seismic data are recorded. Due to the ill-posedness of Equation (3), regularization is needed in order for the establishment of well-posedness to be satisfied. Regularization techniques for a least-squares problem have been extensively studied [9,11,12]. For our problem, we only consider the discrete least-squares problem of Equation (3):

$$\min_{R(\mathbf{x})} \psi(R(\mathbf{x})) := \tfrac{1}{2}\|LR(\mathbf{x}) - \mathbf{d}\|_2^2, \tag{4}$$

where L is the discrete matrix of $\mathcal{L}$. The standard Tikhonov regularization form is given by

$$\min_{R(\mathbf{x})} \Psi(R(\mathbf{x})) := \tfrac{1}{2}\|LR(\mathbf{x}) - \mathbf{d}\|_2^2 + \alpha\Omega(R(\mathbf{x})), \tag{5}$$

where α is the regularization factor which can be chosen by prior information or posterior calculation and $\Omega(R(\mathbf{x}))$ is a function whose role is to give some penalization to the unknown reflectivity function $R(\mathbf{x})$. Just as mentioned in the last section, when the reflection coefficients obey to Gaussian distribution, $\Omega = I$, that is to say $\Omega(R(\mathbf{x})) = \tfrac{1}{2}\|R(\mathbf{x})\|^2$. And it will be like $\Omega(R(\mathbf{x})) = \sum_i \ln(1 + R(\mathbf{x}_i)^2/\sigma^2)$ when they obey Cauchy distribution and $\Omega(R(\mathbf{x})) = \sum_i |R(\mathbf{x}_i)|$ when they obey Laplacian distribution. However, most of the time, the distribution of reflectivity is just impossible to estimate. Therefore, the predefined regularization term may not fit the real situation. Considering this issue, we would like to find the regularization term in other new ways and try to make it have more geological and geophysical meaning.

It is clear that the reflectivity function may be spiky and sparse [16]. We may naturally think about l_0 norm, but because of the numerical infeasibility of the l_0 minimization problem, we relax it to solve the approximation model based on l_1 norm. A simple fact is that the l_1 norm is robust to eliminate outliers and large amplitudes. The presence of the l_1 term also encourages small components of $R(\mathbf{x})$ to become exactly zero, thus promoting sparse solutions. This sounds more meaningful in geology and geophysics. Therefore, in the following, we establish an l_1 norm regularization model for seismic migration inversion:

$$\min_{R(\mathbf{x})} \Psi(R(\mathbf{x})) := \tfrac{1}{2}\|LR(\mathbf{x}) - \mathbf{d}\|_2^2 + \alpha\|R(\mathbf{x})\|_1. \tag{6}$$

All that we perform below are applied to this new model, and its imaging result is compared with other models.

2.1 *Gaussian beam representations of Green's function*

Before proceeding to inversion, we first give out our formulas for Gaussian beam representations of Green's functions in Equation (2). Why we want to do this? The first reason is that the theory that leads to an interpretation of the output in terms of a reflection coefficient breaks down at caustics. This is the so-called caustic problems. The underlying mathematical reason for this is that wave fields are no longer adequately described by a simple amplitude and phase $A \exp\{i\omega\tau\}$ in the neighbourhood of a caustic. In fact, ray theory at this level predicts infinite amplitude at such points while the exact amplitude is finite [8]. In this case, no matter what remedial measures are taken, the interpretation of the peak amplitude of the output on a reflector in terms of the reflection coefficient is no longer valid. To fix this bug in ray-theoretic Green's function, it is best to simply use a better approximation of Green's functions in the processing formulas; integrals over Gaussian beams are one means of providing better quality Green's functions.

The second reason is the problem of multiple arrivals. The form such as $A \exp\{i\omega\tau\}$ can only record one amplitude and one travel time for every shoot–receive pair. However, in practice, there may be several rays that start from the same source point and through the same image point. Integrals over Gaussian beams provide the opportunity to record multiple amplitudes and travel times in multiple Gaussian beams. This makes more sense and approximates the practical scenario better.

We begin with the representation of Green's function in two dimensions (2D). For this case, Green's function with $\mathbf{x}'$ (source point and initial point for the fan of Gaussian beams) and $\mathbf{x}$ (the image point) can be written out as follows:

$$G(\mathbf{x}, \mathbf{x}', \omega) = \frac{i\sqrt{\omega_r w_0^2}}{2v(\mathbf{x}')} \int A_{GB}(\mathbf{x}', \mathbf{x}'') \exp\{i\omega T(\mathbf{x}', \mathbf{x}'')\} \frac{dp_x''}{p_z''}, \tag{7}$$

where

$$A_{GB}(\mathbf{x}', \mathbf{x}'') = \sqrt{\frac{v_0(\mathbf{x}'')}{Q(\mathbf{x}', \mathbf{x}'')}}, \quad T(\mathbf{x}', \mathbf{x}'') = \int_0^s \frac{ds'}{v_0(\mathbf{x}(s'))} + \frac{n^2}{2} \frac{P(\mathbf{x}', \mathbf{x}'')}{Q(\mathbf{x}', \mathbf{x}'')}.$$

The amplitude $A_{GB}(\mathbf{x}', \mathbf{x}'')$ and travel time $T(\mathbf{x}', \mathbf{x}'')$ can be obtained by a ray-tracing technique with a pure imaginary number as the initial value. In the above, ω_r is the reference frequency, and w_0 is the initial half-width of the Gaussian beams. A typical value for ω_r is $2\pi \times 10\,\text{Hz}$, and a typical value for w_0 is one wavelength at the reference frequency. p_x'' is the horizontal slowness and p_z'' is the vertical slowness. P and Q are complex dynamic ray-tracing quantities and are determined along the central ray as solutions of a system of dynamic ray equations. We can refer to [3,8] for more details.

Similarly in 3D cases, Green's function can be asymptotically approximated by the following expression:

$$G(\mathbf{x}, \mathbf{x}', \omega) = \frac{i\omega\omega_r w_0^2}{2\pi v^{3/2}(\mathbf{x}')} \int_{D_\mathbf{x}} A_{GB}(\mathbf{x}', \mathbf{x}'') \exp\{i\omega T(\mathbf{x}', \mathbf{x}'')\} \frac{dp_x'' \, dp_y''}{p_z''}, \tag{8}$$

where

$$A_{GB}(\mathbf{x}', \mathbf{x}'') = \sqrt{\frac{v_0(\mathbf{x}'')}{\det[Q(\mathbf{x}''(s))]}}, \quad T(\mathbf{x}', \mathbf{x}'') = \int_{s_0}^s \frac{ds'}{v_0(\mathbf{x}(s'))} + \frac{1}{2} q^T P Q^{-1} q.$$

Also, the amplitude $A_{GB}(\mathbf{x}', \mathbf{x}'')$ and travel time $T(\mathbf{x}', \mathbf{x}'')$ can be obtained by the 3D ray-tracing technique.

In such a manner, the transition from integral formulas to discrete sums will not lead to evaluations of functions near a zero or infinity in the denominator. We can also record amplitudes and travel times of multiple arrivals in terms of the summation. It is for the inversion formulas that we develop the use of Gaussian beam representations of Green's functions.

2.2 *The gradient and Hessian of the model*

To make it easy to be calculated by computer, we approximate $\|R(\mathbf{x})\|_1$ in Equation (6) by $\sum_{i=1}^{N} \sqrt{(R(\mathbf{x}_i), R(\mathbf{x}_i)) + \epsilon}$, $\epsilon > 0$, and N is the length of the vector $R(\mathbf{x})$. For simplification of notations, we let

$$\Gamma(R(\mathbf{x})) = \left(\frac{R(\mathbf{x}_1)}{\sqrt{R(\mathbf{x}_1)^{\mathrm{T}} R(\mathbf{x}_1) + \epsilon}}, \cdots, \frac{R(\mathbf{x}_i)}{\sqrt{R(\mathbf{x}_i)^{\mathrm{T}} R(\mathbf{x}_i) + \epsilon}}, \cdots, \frac{R(\mathbf{x}_N)}{\sqrt{R(\mathbf{x}_N)^{\mathrm{T}} R(\mathbf{x}_N) + \epsilon}} \right)^{\mathrm{T}}$$

and

$$\Theta(R(\mathbf{x})) = \begin{pmatrix} \frac{\epsilon}{(R(\mathbf{x}_1)^{\mathrm{T}} R(\mathbf{x}_1) + \epsilon)^{3/2}} & 0 & 0 & \cdots & 0 \\ 0 & \ddots & 0 & \vdots & \vdots \\ 0 & \cdots & \frac{\epsilon}{(R(\mathbf{x}_i)^{\mathrm{T}} R(\mathbf{x}_i) + \epsilon)^{3/2}} & \vdots & 0 \\ \vdots & 0 & \vdots & \ddots & \vdots \\ 0 & 0 & \cdots & 0 & \frac{\epsilon}{(R(\mathbf{x}_N)^{\mathrm{T}} R(\mathbf{x}_N) + \epsilon)^{3/2}} \end{pmatrix}.$$

Straightforward calculation yields the gradient of Ψ in migration inversion model (6):

$$g(R(\mathbf{x})) \approx L^{\mathrm{T}}(LR(\mathbf{x}) - \mathbf{d}) + \alpha \Gamma(R(\mathbf{x})), \tag{9}$$

and the Hessian of Ψ in a migration inversion model follows (6):

$$H(R(\mathbf{x})) \approx L^{\mathrm{T}} L + \alpha \Theta(R(\mathbf{x})). \tag{10}$$

With the gradient and Hessian information, the gradient-based iterative methods or the Newton-type methods can be applied. In the following practice, for seismic data with different scales, we will first estimate the product of the number of receivers and the length of each seismic trace and denote it by S. Then, we will choose $\epsilon = S \times 10^{-6}$ empirically.

3. Subspace trust-region method

Research about methods for solving ill-posed seismic migration inversion problems (6) is still very limited. At present, most are based on the inverse Fourier transform or other types of transform [1,4,10,20]. Others included two-step Monte Carlo methods [5], simple least-squares methods [7] and conjugate gradient methods [9,15]. Trust-region methods have been recently shown another useful regularization tool for seismic inversion [19] and have proved to be a kind of regularization method [18]. These methods require solving a trust-region subproblem at every inner iteration and accepting a new trial step within its trust region. Recently, subspace trust-region methods were developed for solving large-scale nonlinear programming problems [13,21], but attentions are paid mainly on well-posed problems. It is clear that these methods have potential applications in seismic migration inversion.

3.1 Subspace trust-region model

Our subspace trust-region model for (6) is

$$\min \quad \Phi_k(\xi) := \mathbf{g_k}^{\mathrm{T}}\xi + \tfrac{1}{2}\xi^{\mathrm{T}}H_k\xi,$$
$$\text{s.t.} \quad \|\xi\| \leq \Delta_k, \tag{11}$$
$$\xi \in S_k,$$

where $\mathbf{g_k} = L^{\mathrm{T}}(LR_k(\mathbf{x}) - \mathbf{d}) + \alpha\Gamma(R_k(\mathbf{x}))$, $H_k = L^{\mathrm{T}}L + \alpha\Theta(R_k(\mathbf{x}))$, Δ_k is the radius of the trust region and S_k is a subspace which is chosen so that (11) can be solved cheaply.

3.2 Solution of a trial step in a 2D subspace trust region

In this subsection, we will give the choice of subspace S_k and an algorithm to solve (11) cheaply [17]. Firstly, the gradient $-\mathbf{g_k}$ should be included in the subspace. Secondly, S_k should contain a sufficiently accurate approximation to the Newton direction $-H_k^{-1}\mathbf{g_k}$. Due to the large scale of the matrix, we should get an inexact Newton step $\mathbf{s_k^N}$ by approximately solving the equation

$$H_k\mathbf{s} = -\mathbf{g_k}$$

with accuracy η_k:

$$H_k\mathbf{s_k^N} = -\mathbf{g_k} + \mathbf{r_k}$$

such that $\|\mathbf{r_k}\|/\|\mathbf{g_k}\| \leq \eta_k$. Hence, we can select S_k as the 2D subspace

$$S_k = \mathrm{span}(\mathbf{s_k^N}, -\mathbf{g_k}).$$

The remaining work is how to solve the subspace trust-region problem (11) efficiently. We define

$$\mathbf{s_1} = \frac{\mathbf{s_k^N}}{\|\mathbf{s_k^N}\|} \tag{12}$$

and compute

$$\mathbf{s_2} = -\mathbf{g_k} + (\mathbf{g_k^T s_1})\mathbf{s_1}, \tag{13}$$

and then we set $\mathbf{s_2} = \mathbf{s_2}/\|\mathbf{s_2}\|$ and $S = [\mathbf{s_1}, \mathbf{s_2}] \in \mathbb{R}^{N^2 \times 2}$. Then, for any vector $\mathbf{s} \in S_k$, there exists a 2D vector $\boldsymbol{\beta} = [\beta_1, \beta_2]^{\mathrm{T}} \in \mathbb{R}^2$ that satisfies $\mathbf{s} = S\boldsymbol{\beta}$. Hence, problem (11) can be formulated as a 2D trust-region subproblem:

$$\min \quad \Phi(\boldsymbol{\beta}) := \mathbf{g_k^T}S\boldsymbol{\beta} + \tfrac{1}{2}\boldsymbol{\beta}^{\mathrm{T}}S^{\mathrm{T}}H_kS\boldsymbol{\beta},$$
$$\text{s.t.} \quad \|S\boldsymbol{\beta}\| \leq \Delta_k. \tag{14}$$

With the above description, we can present the following algorithm for solving the subspace trust-region model (11) in detail.

ALGORITHM 1 *Solving the subspace trust-region problem*

Step 1. *Compute* $\mathbf{s_1}$ *and* $\mathbf{s_2}$ *by* (12) *and* (13), *respectively.*
Step 2. *Set* $\mathbf{s_2} = \mathbf{s_2}/\|\mathbf{s_2}\|$ *and* $S = [\mathbf{s_1}, \mathbf{s_2}] \in \mathbb{R}^{N^2 \times 2}$.
Step 3. *Solve the 2D trust-region subproblem* (1) *to get* $\boldsymbol{\beta}$.
Step 4. *Set* $\boldsymbol{\xi_k} = S\boldsymbol{\beta}$ *to be the solution of model* (11).

3.3 *A subspace trust-region method*

Generally, a trust-region algorithm uses

$$r_k = \frac{\text{Ared}_k}{\text{Pred}_k}$$

to decide whether the trial step ξ_k is acceptable and how the next trust-region radius is chosen, where

$$\text{Pred}_k = \Phi_k(0) - \Phi_k(\boldsymbol{\xi_k})$$

is the predicted reduction in the approximate model, and

$$\text{Ared}k = \psi(\mathbf{R_k}) - \psi(\mathbf{R_k} + \boldsymbol{\xi_k})$$

is the actual reduction in the objective functional.

Based on these definitions, we give the subspace trust-region algorithm for seismic migration inversion.

ALGORITHM 2 *A subspace trust-region algorithm for seismic migration inversion*

Step 1. *Choose parameters* $0 < \tau_3 < \tau_4 < 1 < \tau_1, 0 \leq \tau_0 \leq \tau_2 < 1, \tau_2 > 0$ *and initial values* $\mathbf{R_0}, \Delta_0 > 0$. *Set* $k := 1$.

Step 2. *If the stopping rule is satisfied then STOP*; *else, use Algorithm* 1 *to solve problem* (11) *to get* $\boldsymbol{\xi}_k$.

Step 3. *Compute* r_k.

$$\mathbf{R_{k+1}} = \begin{cases} \mathbf{R_k}, & \textit{if } r_k \leq \tau_0. \\ \mathbf{R_k} + \boldsymbol{\xi_k}, & \textit{otherwise.} \end{cases} \qquad \begin{matrix} (15) \\ (15') \end{matrix}$$

Choose Δ_{k+1} *that satisfies*

$$\Delta_{k+1} \in \begin{cases} (\tau_3 \|\boldsymbol{\xi_k}\|, \tau_4 \Delta_k), & \textit{if } r_k < \tau_2, \\ (\Delta_k, \tau_1 \Delta_k), & \textit{otherwise.} \end{cases} \qquad \begin{matrix} (16) \\ (16') \end{matrix}$$

Step 4. *Evaluate* $\mathbf{g_k}$ *and* H_k; $k := k + 1$. *Goto Step* 2.

4. Numerical examples

To show the advantage of the proposed new method, in this section, we would like to compare it with the three most popular methods which are being used in seismic migration inversion.

4.1 *1D model*

Suppose the velocity profile under a source point is as shown in Figure 1. Thus, it has a reflector with reflectivity 0.1111 at the depth 500 m, also 0.0909 at 800 m, 0.0769 at 1200 m and 0.0667 at 1600 m, respectively. In traditional methods, they usually adopt Green's function of constant velocity and use FFT to accelerate the inversion. Figure 2(a) shows the result of this kind of method. We can see that, this method can only achieve proper reflectivity when the depth is not very large. With the depth increasing, its error in both amplitude and position will become larger and larger. If we get more exact Green's function using ray tracing and use the proposed method in this paper to perform the inversion, the imaging result will be much better, which is shown in Figure 2(b). Both the amplitudes and the positions are well inverted in Figure 2(b).
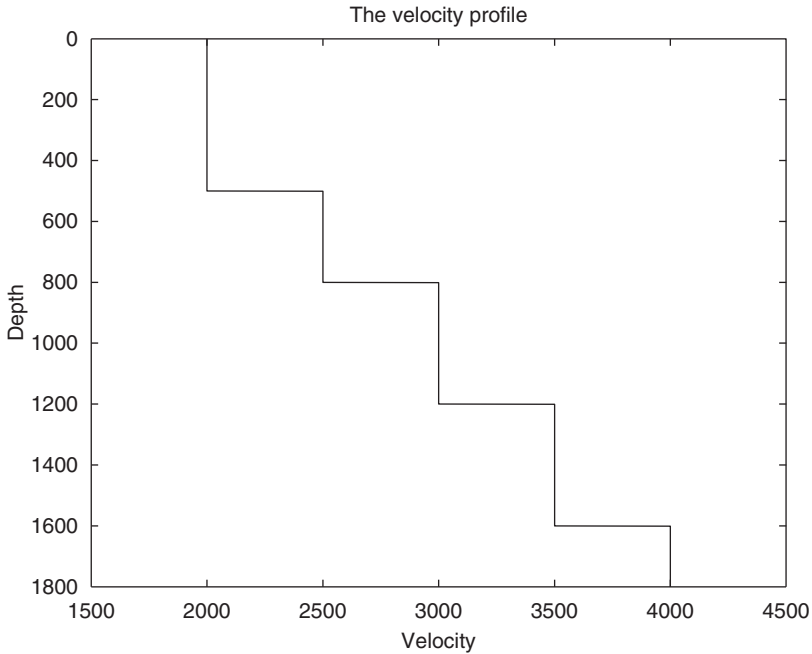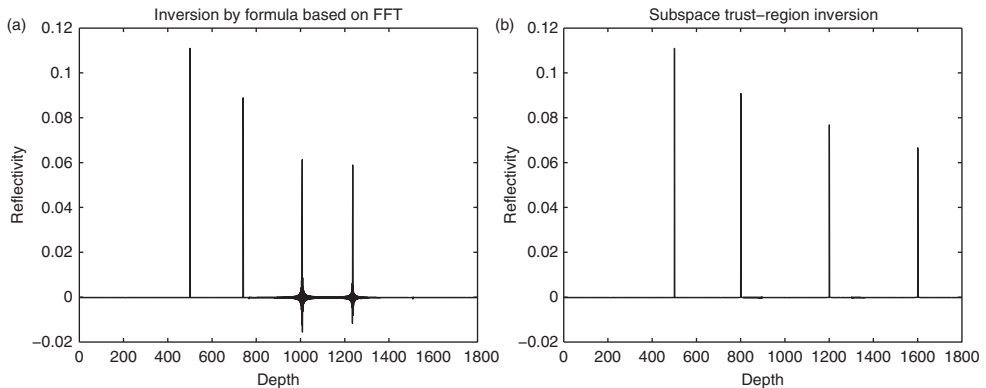
Figure 1.   1D velocity profile.

Figure 2.   Fast transform inversion (a) and subspace trust-region migration inversion (b).

4.2   *Fault model*

Next, we will confirm the validity of the new algorithm to a fault model which is a common type of structure. The velocities for the three layers in Figure 3 are 2000, 2500 and 3000 m/s from top to bottom; 101×101 grids are adopted in the experiment, the offset is 40 m and the temporal sampling is 0.002 s. The noise level is 0.01 in this experiment. Firstly, we apply Kirchhoff migration to the synthetic data. Kirchhoff migration is the most popular method which is being used in the oil exploration industry, because it is very fast. It uses the conjugate operator to approximate the inverse of the forward modelling operator, then does the inversion inexactly but efficiently. Figure 4(a) and (b) shows the result of Kirchhoff poststack time migration and subspace trust-region migration inversion, respectively. It takes 0.89 and 4.83 s to perform the
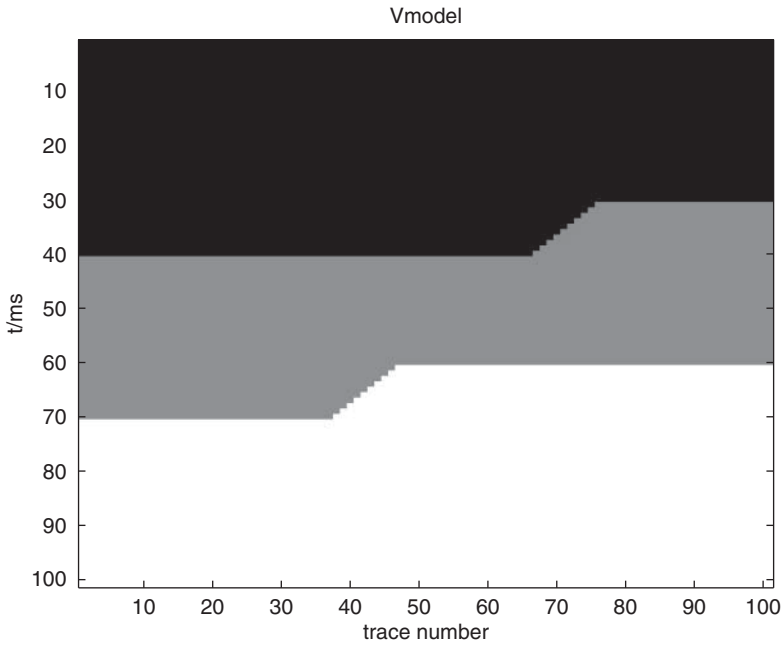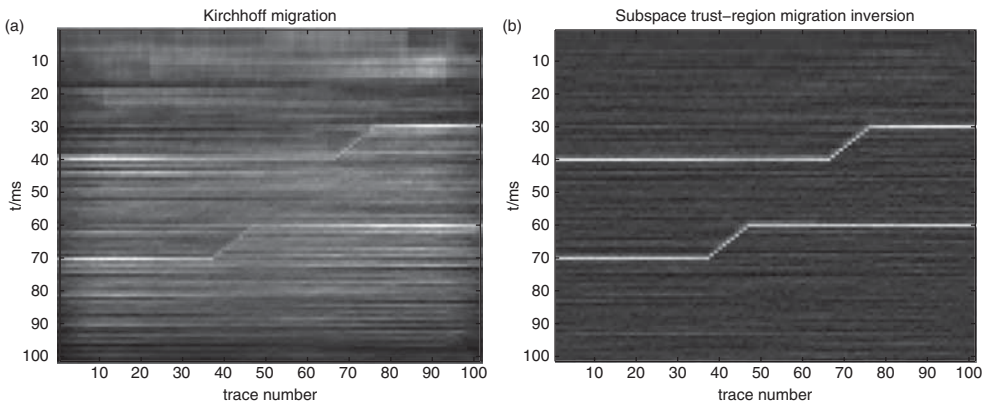
Figure 3. Fault velocity model.

Figure 4. Kirchhoff migration (a) and subspace trust-region migration inversion (b).

migration, respectively. We can find that Kirchhoff migration only gives a blurred image, while the latter one gives a very clear one, although the subspace trust-region method consumes more time. The total computation amount of Kirchhoff migration is as much as that of one iteration in the subspace trust-region method.

4.3 *Marmousi model*

Finally, let us come to a very familiar example in geophysics – the Marmousi model. This model is extensively used to test the effectiveness of migration algorithms. We use a 122×384 sampled grid version of these data. Solving the migration inversion model (4) yields the least-squares migration method. And our method is applying the subspace trust-region method to solve migration inversion
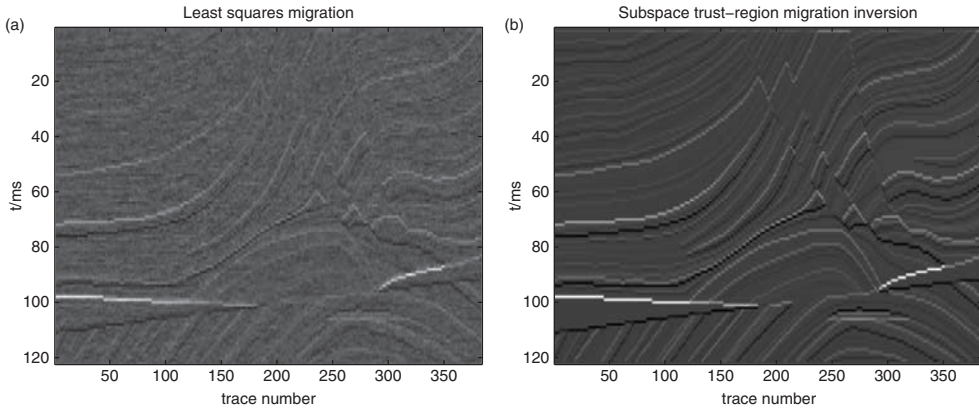
Figure 5.   Least-squares migration (a) and subspace trust-region migration inversion (b).

model (6). Figure 5(a) and (b) shows the result of least-squares migration and subspace trust-region migration inversion, respectively. By comparing the imaging quality in the two figures, we can discover that the resolution of our method is higher than that of the least-squares migration method. Moreover, since we use the subspace technique to accelerate our method, we spend less time than most least-squares migration methods. In this test case, our method takes 12.62 s, while a projected BB (Barzilar-Borwein) method, which is a very efficient method to solve least-square problems, takes 14.32 s.

4.4   *Discussion*

In this section, we find that the proposed method in this paper behaves better than many popular migration algorithms. However, this is not enough. There are still several further research issues for improvement, such as applying it to various seismic forward models, refining the forward matrix by proper preconditioners, etc. Although this algorithm takes much more time than the traditional Kirchhoff migration, its duration of calculation may be reduced a lot by designing parallel computation algorithms, or we can concentrate our method only on the area we are interested in (such as thin reservoir), and this can also apparently reduce computational complexity.

5.   Conclusion

Regularized seismic migration inversion is a relatively new field which is worthy of exploration. There is wide space for the application of good inversion algorithms. In this paper, we formulated Green's function in a new way and investigated a new method to solve seismic migration inversion problems by applying a trust-region technique. The method applied a subspace technique to the trust-region subproblem, which possesses not only the efficiency but also the global convergence.

The results of numerical experiments showed that the migration inversion method proposed in this paper can yield images with true amplitude and better resolution. Therefore, we concluded that our proposed algorithm is applicable for seismic migration inversion problems.

Acknowledgements

References

[1] W.B. Beydoun, J. Delvaux, M. Mendes, G. Noual, and A. Tarantola, *Practical aspects of an elastic migration/inversion of crosshole data for reservoir characterization: A Paris Basin example*, Geophysics 54(12) (1989), pp. 1587–1595.
[2] N. Bleistein, J.K. Cohen, and W. Stockwell, *Mathematics of Multidimensional Seismic Imaging, Migration, and Inversion*, Springer, New York, 2000.
[3] S.H. Gray and N. Bleistein, *True-amplitude Gaussian-beam migration*, Geophysics 74(02) (2009), pp. S11–S23.
[4] M.V. de Hoop, B. Robert, S. Carl and D. Miller, *Generalized radon transform/amplitude versus angle (GRT/AVA) migration/inversion in anisotropic media*, Proc. SPIE 15 (1994), pp. 2301.
[5] S. Jin and R. Madariaga, *Nonlinear velocity inversion by a two-step Monte Carlo method*, Geophysics 59 (1994), pp. 577.
[6] C. Lanczos, *Linear Differential Operators*, Van Nostrand, London, 1961, pp. 120–124.
[7] T. Nemeth, C.J. Wu, and G.T. Schuster, *Least-squares migration of incomplete reflection data*, Geophysics 64(1) (1999), pp. 208–221.
[8] M.M. Popov, *Ray Theory and Gaussian Beam Method for Geophysicists*, EDUFBA, Salvador, 2002.
[9] M.D. Sacchi, J.F. Wang, and H. Kuehl, *Regularized Migration/Inversion: New Generation of Seismic Imaging Algorithm*, CSEG Recorder, 2006 Special Edition, Canadian Society of Exploration Geophysicists, Calgary, pp. 54–59.
[10] R.H. Stolt and A.B. Weglein, *Migration and inversion of seismic data*, Geophysics 50(12) (1985), pp. 2458–2472.
[11] A.N. Tikhonov and V.Y. Arsenin, *Solutions of Ill-Posed Problems*, John Wiley and Sons, New York, 1977.
[12] C.R. Vogel, *Computational Methods for Inverse Problems*, SIAM, Philadelphia, PA, 2002.
[13] Y.F. Wang, *Computational Methods for Inverse Problem and Their Applications (New Frontiers of Sciences)*, Higher Education Press, Beijing, 2007 (in Chinese).
[14] Y.F. Wang, *On iterative regularization methods for migration deconvolution and inversion in seismic imaging*, Chinese J. Geophys. 52(3) (2009), pp. 704–715.
[15] Y.F. Wang, *Accelerating migration deconvolution using a nonmonotone gradient method*, Geophysics 75(4) (2010), pp. 131–137.
[16] Y.F. Wang, *Seismic impedance inversion using l_1-norm regularization and gradient descent methods*, J. Inverse Ill-posed Probl. 18 (2011), pp. 823–838.
[17] Y.F. Wang and S.Q. Ma, *A fast subspace method for image deblurring*, Appl. Math. Comput. 215(6) (2009), pp. 2359–2377.
[18] Y.F. Wang and Y.X. Yuan, *Convergence and regularity of trust region methods for nonlinear ill-posed inverse problems*, Inverse Probl. 21 (2005), pp. 821–838.
[19] Y.F. Wang, J.J. Cao, and C.C. Yang, *Recovery of seismic wavefields based on compressive sensing by an l_1-norm constrained trust region method and the piecewise random sub-sampling*, Geophys. J. Int. 187 (2011), pp. 199–213.
[20] S. Xu and L. Gilles, *Fast migration/inversion with multivalued rayfields: Part I method, validation test, and application in 2D to Marmousi*, Geophysics 69(5) (2004), pp. 1311–1319
[21] Y.X. Yuan, *Numerical Methods for Nonlinear Programming*, Shanghai Scientific and Technical Publishers, Shanghai, 1993 (in Chinese).